Research Square

Preprints are preliminary reports that have not undergone peer review.
They should not be considered conclusive, used to inform clinical practice,
or referenced by the media as validated information.

# MRE11A Regulates Sepsis Through the mtDNA/STING Pathway of T Lymphocyte Apoptosis

**Zhixin Wei**
The First Affiliated Hospital of Guangxi Medical University
**Feifei Wang**
The First Affiliated Hospital of Guangxi Medical University
**Pengji Qin**
The First Affiliated Hospital of Guangxi Medical University
**Zhiyong Yang**
Yangzhiyong@gxmu.edu.cn
The First Affiliated Hospital of Guangxi Medical University

**Research Article**

**Keywords:** meiosis-related recombination 11 homolog A, sepsis, T lymphocytes, apoptosis, cGAS/STING pathway

**Posted Date:** April 24th, 2026

**DOI:** https://doi.org/10.21203/rs.3.rs-9414184/v1

**License:** This work is licensed under a Creative Commons Attribution 4.0 International License.
Read Full License

**Additional Declarations:** No competing interests reported.

MRE11A Regulates Sepsis Through the mtDNA/STING Pathway of T Lymphocyte Apoptosis

**Authors:** First Author: Zhixin Wei (mailto:WZX990422@163.com)

Second Author: Feifei Wang (mailto:202320132@sr.gxmu.edu.cn)

Third Author: Pengji Qin (mailto:15086039572@163.com)

Corresponding Author: Zhiyong Yang

(mailto:Yangzhiyong@gxmu.edu.cn)

**Affiliations:** All authors are affiliated with the Pediatric Intensive Care Unit (PICU), Guangxi Clinical Research Center for Pediatric Diseases, The First Affiliated Hospital of Guangxi Medical University, Nanning, Guangxi, China.

**Corresponding Author:** Zhiyong Yang

Email: mailto:Yangzhiyong@gxmu.edu.cn

Address: Pediatric Intensive Care Unit (PICU), Guangxi Clinical Research Center for Pediatric Diseases, The First Affiliated Hospital of Guangxi Medical University, Nanning, Guangxi, China.

**Funding:** This research was funded by the Guangxi Clinical Research Center for Pediatric Diseases (Project No. GUIKEAD22035219) and the Guangxi Natural Science Foundation General Program (Project No. 2024GXNSFAA010084).

**Conflict of Interest:** The authors declare that the research was conducted in the absence of any commercial or financial relationships that could be

construed as a potential conflict of interest.

**Author Contributions:** ZW (Zhixin Wei): Writing – original draft.

FW (Feifei Wang): Data curation, Writing – original draft.

QP(Peng ji Qin): Experimental design – original draft.

ZY (Zhiyong Yang): Writing – review & editing.

**Acknowledgements:** Guangxi Clinical Research Center for Pediatric Diseases

## Abstract

**Objective and Significance:** To analyze changes in meiosis-related recombination homolog 11A (MRE11A) expression in T lymphocytes from pediatric sepsis patients and mouse models, and to explore the potential regulatory mechanisms of MRE11A in sepsis.

**Methods:** Flow cytometry was employed to detect MRE11A expression levels and the expression of the apoptosis-related molecule Cleaved Caspase-3 in peripheral blood T lymphocytes from 20 pediatric sepsis patients and 20 healthy control children.

A mouse sepsis model was established via cecal ligation and puncture (CLP). Sepsis mice were treated at 24h, 48h, and 72h post-CLP. Intraperitoneal injection of the MRE11A inhibitor Mirin simulated reduced MRE11A expression in mice; Mirin-treated mice underwent processing 24h after inhibitor administration.CD3+ T cells were isolated from mouse spleens. Immunofluorescence was used to detect MRE11A expression in T lymphocyte cytoplasm. Real-time quantitative polymerase chain reaction (qPCR) assessed changes in mitochondrial DNA (mtDNA) within T lymphocyte cytoplasm. qPCR and Western blot (WB) analysis examined T lymphocyte expression of STING pathway-related factors cGAS,STING, and apoptosis-related factors , Cleaved Caspase-3 , and Bax.

**Results:**In the sepsis group, the proportion and expression levels of CD4+MRE11A+T cells and CD8+MRE11A+T cells were lower than those in the control group. The proportions of CD4+Cleaved caspase-3+T cells and CD8+Cleaved caspase-3+T cells were higher in the sepsis group than in the control group, with statistically significant differences between the two groups (both $P < 0.05$). MRE11A expression decreased in T cells from both the sepsis group (CLP24h, CLP72h) and the Mirin group, while mtDNA expression was upregulated (both $P < 0.05$).cGAS expression increased in T cells from sepsis group mice (CLP24h) and Mirin group mice, while STING expression was up-regulated in T cells from CLP48h and Mirin groups (all $P < 0.05$);T cells from the sepsis group (CLP24h, CLP48h) and Mirin group showed increased Cleaved Caspase-3 expression, while Bax expression was upregulated in CLP24h group T cells (all $P < 0.05$).

Conclusions: MRE11A cytoplasmic expression was reduced in T lymphocytes from

pediatric sepsis patients, potentially associated with T lymphocyte apoptosis. Low MRE11A expression in mouse sepsis T lymphocytes may induce mtDNA leakage, participating in T lymphocyte apoptosis by activating the cGAS/STING pathway.MRE11A may represent a novel therapeutic target for clinical treatment of sepsis.

Keywords: meiosis-related recombination 11 homolog A; sepsis; T lymphocytes; apoptosis; cGAS/STING pathway

## Introduction

Sepsis is a life-threatening organ dysfunction caused by infection-induced dysregulation of the host immune system, ranking among the primary conditions consuming pediatric critical care resources globally[1] .Global epidemiological studies indicate that approximately 25 million children worldwide contracted sepsis in 2017, with 3 million cases resulting in sepsis-related deaths. Between 2016 and 2020, sepsis was the leading direct cause of death among children under five, accounting for 36.7% of fatalities[2] .Immunological mechanisms play a crucial role in the pathophysiology of sepsis. Immunosuppression is a key factor leading to secondary infections and contributes significantly to the poor prognosis of sepsis patients[3] . Elucidating the mechanisms underlying sepsis-related immune dysfunction and identifying novel immunotherapeutic targets for sepsis are current research priorities.

Previous studies have demonstrated that abnormal apoptosis of immune cells is a major cause of sepsis-associated immunosuppression, with T lymphocytes playing a crucial role in the immune mechanisms of sepsis. Elevated apoptosis levels in T cells and B cells lead to T lymphocyte (hereinafter referred to as T cell) exhaustion[4,5] .When T cell numbers decrease and functional impairment occurs, it further induces an immunosuppressive state. The exacerbation of immunosuppression is closely associated with increased mortality in sepsis patients[6] . In the pathological progression of sepsis, T cell apoptosis is one of the key factors contributing to sepsis-associated lymphopenia.A comparative autopsy study between fatal sepsis patients and non-

infectious cause deaths revealed significantly reduced T cell counts in the spleens of fatal sepsis patients[7] . The pathophysiological significance of heightened apoptosis in sepsis has now been validated in animal models.Multiple related studies indicate that intervening to inhibit apoptosis significantly improves survival rates in experimental subjects[8–11] . Furthermore, research on COVID-19 has also identified that mitochondrial DNA damage in $CD3^+$T cells can induce apoptosis[10] .

Meiotic recombination 11 homolog A (MRE11A) is a protein closely associated with double-stranded DNA (dsDNA) break repair, homologous recombination activity, and telomere length maintenance. Its primary localization is the cell nucleus, and this protein possesses 3'→5' exonuclease activity and endonuclease activity.Upon binding to DNA, the nuclease functional domain of MRE11A is exposed, forming a channel that facilitates DNA cleavage activity. This enables the execution of nuclease-catalyzed reactions at DNA termini[11] .Additionally, MRE11A has been found in the cytoplasm, where it binds to mitochondrial DNA (mtDNA) to maintain mitochondrial genome integrity[12] .In a series of studies on rheumatoid arthritis, T lymphocytes lacking MRE11A prematurely aged . Defective MRE11A in T cells causes mitochondrial damage, leading to impaired mtDNA repair. This repair abnormality ultimately results in mtDNA leakage from mitochondria into the cytoplasm[6] .Cyclic guanosine monophosphate-adenosine monophosphate synthase (cGAS) functions as an intracellular DNA sensor. Within the cytoplasm, mtDNA can bind to cGAS, forming cyclic guanosine monophosphate-adenosine monophosphate (cGAMP).cGAMP). cGAMP binds to the stimulator of interferon genes (STING) on the endoplasmic reticulum, activating STING and subsequently initiating innate immune responses and tumor suppression[13] .Recent studies indicate that MRE11 dissociates cGAS from histone acidic fragments by binding the MRE11-RAD50-NBN (MRN) complex to nucleosome fragments, thereby enabling recognition and response to endogenous DNA damage[14] .

STING promotes T cell apoptosis by regulating calcium ion ($Ca^{2+}$) homeostasis and endoplasmic reticulum stress· .Caspase-3 is a key executor of apoptosis. On one hand, it directly induces cell death by cleaving downstream substrates; on the other

hand, increased expression of pro-apoptotic proteins (e.g., Bax) and decreased expression of anti-apoptotic proteins (e.g., Bcl-2) activate Caspase-3, further amplifying the apoptotic signal[16] .Cleaved caspase-3, the active form of caspase-3, serves as the terminal effector enzyme in apoptosis, directly participating in the core mechanism of cell killing. Multiple studies have demonstrated significantly elevated caspase-3 expression in sepsis patients and animal models[17,18] .However, our understanding of MRE11A's role in T-cell apoptosis during sepsis remains limited. Based on the above studies, MRE11A, as an mtDNA repair enzyme, may inhibit apoptosis by protecting mitochondria.Nevertheless, gaps remain in the study of MRE11A in sepsis. Therefore, this study combines clinical data with animal experiments to investigate for the first time the correlation between MRE11A expression, mitochondrial changes, and T-cell apoptosis. The aim is to provide new theoretical support for clinical interventions targeting lymphopenia in sepsis and improving patient prognosis.

# Methods

## Clinical Study Subjects

Clinical data were collected from 20 pediatric patients with sepsis admitted to the PICU of the First Affiliated Hospital of Guangxi Medical University between

January 2020 and October 2022. Inclusion criteria: aged 1 month to 18 years, meeting the diagnostic criteria established by the 2005 International Pediatric Sepsis Consensus Conference.Exclusion criteria: PICU admission duration < 24 hours; severe medical record deficiencies. Concurrently, 20 healthy children undergoing outpatient physical examinations at the same hospital served as controls, excluding those with infections, immune dysfunction, or organic diseases. This study was approved by the Ethics Committee of the First Affiliated Hospital of Guangxi Medical University (Ethics No.: 2023-E031-01).

**Flow Cytometry Analysis**

Peripheral blood (5 mL) was collected within 24 hours of admission from pediatric sepsis patients and healthy controls, anticoagulated with sodium heparin. Peripheral blood mononuclear cells (PBMCs) were isolated using density gradient centrifugation.A flow cytometer was used to detect MRE11A expression (mean fluorescence intensity [MFI] and percentage of positive cells) in CD4+ T cells and CD8+ T cells, as well as the percentage of cells positive for cleaved caspase-3. The antibodies and reagents used are listed in Table 1.

**Animals and Ethics**

Healthy male C57BL/6 mice (7–9 weeks old, 18–22 g) were purchased from the Experimental Animal Center of Guangxi Medical University.Mice were housed in a 12-hour light/dark cycle under SPF barrier conditions with free access to food and water. All procedures adhered to NIH guidelines and were approved by the Ethics Committee of the First Affiliated Hospital of Guangxi Medical University (Ethics No.: 2023-E031-01). Antibodies and reagents used are listed in Table 1.

**Cecal Ligation and Perforation (CLP) Model**

This study employed the cecal ligation and puncture (CLP) technique to establish an animal model of sepsis. Animals were anesthetized with inhaled isoflurane at a concentration of 1.5%. Following successful anesthesia, the abdominal skin was disinfected three times with povidone-iodine. A midline abdominal incision approximately 2 cm in length was made to open the abdominal cavity. The cecum was identified,Carefully dissect its distal mesentery from the large intestine. Tightly ligate

the distal half of the cecum with sterile 4-0 silk suture. Using a sterile 25-gauge needle, perform a central transection puncture at the ligated distal cecum. Gently expel a small amount of intestinal contents while minimizing vascular damage. Then reposition the cecum into the abdominal cavity and close the incision.

**Experimental Groups and Treatment Methods**

Sepsis-induced mice underwent treatment at 24h, 48h, and 72h, with 6 mice per group. The MRE11A inhibitor Mirin was administered via intraperitoneal injection to simulate reduced MRE11A levels in mice. Mirin was injected at 25 mg/kg body weight ( ) intraperitoneally. Injections were administered once daily for 3 consecutive days. Mice in the Mirin group underwent treatment 24 hours after completion of inhibitor injections.

**Histological Analysis**

Lung tissue was excised, fixed in 4% paraformaldehyde solution, and dehydrated using ethanol at varying concentrations (70%-100%).Tissues were paraffin-embedded, sectioned at 5 μm thickness, and subjected to histopathological evaluation using hematoxylin-eosin staining. HE-stained sections served as reference for scoring based on five pathological criteria: exudate, congestion, alveolar hemorrhage and tissue debris, neutrophil infiltration, and cytopathic hyperplasia.No relevant pathological findings scored 0 points; mild pathological changes scored 1 point; moderate pathological changes scored 2 points; and severe pathological changes scored 3 points. The sum of the five scores constituted the lung tissue injury score[19] .

**Assessment of General Mouse Condition**

Scoring is based on the MSS criteria established by Bradley Shrum et al. in 2014[20] . Seven observation criteria are assessed: appearance, eye opening and discharge, reduction in spontaneous activity and its degree, altered consciousness, respiratory rate, respiratory quality, and response to stimuli. Each criterion is graded on a 5-point scale (0–4 points).The total score for each mouse was the sum of the seven indicators, with a maximum score of 28 points. Dead mice were assigned the maximum score.

**ELISA assay for inflammatory cytokine IL-6 in peripheral blood serum**

Blood samples were collected from the retroorbital venous plexus, centrifuged at 1,000 rpm for 10 minutes, and serum was extracted. Serum IL-6 levels were measured using an ELISA kit.

**Extraction of PBMCs and T cells from mouse spleen**

Place mouse spleen on a 200-mesh sieve and grind until no visible red lumps remain. Rinse the sieve with PBS, centrifuge at 300 g for 5 min, and discard the supernatant. Resuspend cells in 1× red blood cell lysis buffer, incubate at room temperature for 2–3 min to lyse, then add 10 mL PBS. Centrifuge at 300 g for 5 min and discard the supernatant.Resuspend spleen cells in PBS. Isolate mouse spleen PBMCs according to the mouse lymphocyte isolation kit instructions. Count cells using a cell counter and adjust to$^{1\times10^8}$cells/mL for subsequent experiments.

Take a 5 mL polystyrene round-bottom tube and add 1 mL of mouse spleen PBMC sample. Add 50 μL Rat Serum to the sample. Add 50 μL Isolation Cocktail to the sample, mix well, and incubate at room temperature for 10 min. Vortex RapidSpheres™ for 30 seconds, add 75 μL RapidSpheres™ to the sample, mix well, and incubate at room temperature for 2.5 min.Add $Ca^{2+/Mg^{2+}\text{-free}}$, phenol red-free 1× Hanks' BSS to a final volume of 2.5 mL ( ). Gently pipette up and down 2-3 times to mix. Place the tube on a magnet and incubate at room temperature for 2.5 min.Remove the magnet and transfer the enriched cell suspension to a new tube to obtain a $CD3^+$Tcell suspension. Count the cells using a cell counter and adjust to$^{1\times10^6}$cells/mL for subsequent experiments.

**Extraction and Purification of T Cell Cytoplasmic mtDNA**

Separate T cell cytoplasm using the Biyuntian Cytoplasmic Protein Extraction Kit, then purify cytoplasmic mtDNA with the Tiangen Free DNA Extraction Kit. Assess DNA concentration and purity using NanoDrop2000 (Thermo).

**Immunofluorescence Analysis**

Paraffin-embedded spleen tissue sections underwent dewaxing and rehydration, followed by antigen retrieval with pH 8.0 EDTA alkaline solution. Sections were blocked with 3% hydrogen peroxide solution at room temperature for 15 min, then incubated with 5% goat serum at room temperature for 30 min. Primary antibodies CD3

and MRE11A were applied to sections and incubated overnight at 4°C.After washing with PBS, anti-rabbit/mouse secondary antibody for immunohistochemistry was added and incubated at room temperature for 30 min. TSA fluorescent dye was used for color development. Cell nuclei were stained with DAPI, and fluorescent images were captured using a fluorescence microscope.

**Real-time quantitative PCR**

Quantification of mtDNA levels, STING pathway-related factors cGAS and STING, as well as apoptosis-related factors Cleaved Caspase-3 and Bax was performed via real-time polymerase chain reaction. β-Actin served as the internal reference gene for amplification. Primer sequences for these assays are listed in the table. Relative expression levels were calculated using the 2^(△△CT) method. Primer sequences used are shown in Table 2.

**Western Blotting**

Spleen tissue samples were rapidly frozen in liquid nitrogen and then lysed in RIPA buffer containing protease and phosphatase inhibitors. Lysates were centrifuged at 13,000g for 15 minutes, and the supernatant was collected.Protein concentration was measured using a BCA protein assay kit. Equal amounts of protein were separated on an 8-12% SDS-PAGE gel and transferred to a PVDF membrane. The membrane was blocked with 5% nonfat milk in TBS containing 0.1% Tween-20 for 1 hour, then incubated overnight at 4°C with the primary antibody.After washing, membranes were incubated with HRP-labeled secondary antibody at room temperature for 1 hour. Optical density analysis was performed using Image J.

**Statistical Analysis**

Statistical analysis was performed using SPSS 27.0 software, and graphs were generated using Prism GraphPad 8.0 software.Normally distributed quantitative data are expressed as mean ± standard deviation (Mean ± SD). Comparisons between two groups were performed using the independent samples t-test. Comparisons among multiple groups were performed using one-way ANOVA. If the homogeneity of variance test yielded a P- >0.05, the Least Significant Difference (LSD) test was selected. If the homogeneity of variance test yielded a P<0.05, the Tamarind test was

selected.Non-normally distributed quantitative data were expressed as median and interquartile range [M (P25, P75)]. Comparisons between two groups were performed using the two-sample rank-sum test, while comparisons among multiple groups were conducted using the Kruskal-Wallis test. Count data were presented as cases (%). $P < 0.05$ was considered statistically significant.

Table 1 Antibodies and Chemical Reagents

| Reagent Consumables | Company | Source |
|---|---|---|
| APC anti-human CD3 | Biolegend | United States |
| Brilliant Violet 650 anti-human CD3 | Biolegend | United States |
| PE anti-human CD4 | Biolegend | United States |
| Mre11 Ab (15B8.1E7.6) [Alexa Fluor® 405 | Novus | United States |
| FITC Rabbit Anti-Active Caspase-3 | Becton, Dickinson and Company | USA |
| APC-H7 Mouse Anti-Human CD4 | Becton, Dickinson and Company | United States |
| BV605 Mouse Anti-Human CD8 Clone SK1 (RUO) | Becton, Dickinson and Company | United States |
| Hu/NHP CD3 R718 SP34-2 | Becton, Dickinson and Company | United States |
| Cyto-Fast™ Fix/Perm Buffer Set | Biolegend | United States |
| True-Nuclear™ Transcription | Novus | USA |
| Mouse IL-6 ELISA Kit | Lianke Bio | China |
| Mouse Lymphocyte Isolation Kit | SolaBio | China |
| EasySep Mouse T Cell Isolation Kit | STEMCELL | Canada |
| EasySep Violet Magnet | STEMCELL | Canada |
| Cell Adhesion Mediator | Prelay | China |
| Rabbit polyclonal antibody to Mre11 | Affinity | United States |
| Anti-rabbit Alexa Fluor 488 | Biyuntian | China |
| DAPI | Biyuntian | China |
| PMSF | Blue Sky | China |

| | | |
|---|---|---|
| HiPure Total RNA Mini Kit | Meiji Bio | China |
| Free DNA Extraction Kit | Tiangen | China |
| Nuclear and Cytoplasmic Protein Extraction Kit | Biyuntian | China |
| Fast First-Strand cDNA Synthesis Mix for RT (with dsDNase) | Albatross Goonie | China |
| qPCR SYBR Green Fast Taq Mix | Albatross Goonie | China |
| Primer | Shanghai Sangon | China |

Table 2 All primer sequence information

| Gene | Forward primer，5’-3’ | Reverse primer，5’-3’ |
|---|---|---|
| β-Actin | GTGACGTTGACATCCGTAAAGA | GTAACAGTCCGCCTAGAAGCAC |
| MT-ND1 | TGGTCCATACGGCATTTTAC | TTGGTAGGGGAACTCATAGA |
| Cleaved Caspase-3 | AGCACCTGGTTACTATTCCTGGAG | GGATCTGTTTCTTTGCGTGGA |
| Bax | TGAGCGGCTGCTTGTCTGG | GGTGAGCGAGGCGGTGAG |
| cGAS | GGCACAAAAGTGAGGACCAATC | GATTCACAGCATGTTTTCTCTATCC |
| STING | TCGGGTTTATTCCAACAGCG | GTTTAGCCTGCTCAAGCCGAT |

# Results

## Expression of MRE11A and Cleaved Caspase-3 in T Cells of Pediatric Sepsis Patients

Flow cytometry analysis revealed that the proportion and expression levels of $CD4^+MRE11A^+$T cells and $CD8^+MRE11A^+$T cells were significantly lower in the sepsis group compared to the control group.Concurrently, the proportions of Cleaved Caspase-3-positive $CD4^+$T cells and $CD8^+$T cells in the sepsis group were significantly higher than those in the healthy control group (both $P < 0.05$). See Table 3 and Figure 1 for details.

Table 3 Comparison of MRE11A and Cleaved Caspase-3 Expression in the Cytoplasm of T Lymphocytes Between the Sepsis Group and Control Group

| | Sepsis group (n=20) | Control group (n=20) | Z-value | *P*- -value |
|---|---|---|---|---|
| $CD4^+$ $MRE11A^+$ T-cell proportion (%) | 3.91 (2.29, 9.73) | 99.90 (97.55, 99.99) | -5.413 | <0.001 |
| $CD4^+$ MRE11A expression levels (MFI) in T cells | 1665.16 (1556.86, 1802.15) | 5689.04 (4388.69, 9567.34) | -5.410 | <0.001 |
| $CD8^+MRE11A^+$T-cell ratio (%) | 4.09 (2.00, 9.58) | 92.15 (76.73, 96.39) | -5.302 | <0.001 |
| $CD8^+$ MRE11A expression levels (MFI) in T cells | 1921.82 (1737.61, 2164.92) | 4164.97 (2,894.47, 9,122.24) | -4.586 | <0.001 |
| $CD4^+$Cleaved Caspase-$3^+$T-cell ratio (%) | 1.34 (1.06, 2.23) | 0.13 (0.03, 0.67) | -4.384 | <0.001 |
| Cleaved Caspase-3 Expression Level (MFI) in $CD4^+$T Cells | 2259.86 (2029.88, 2710.46) | 2546.17 (2219.4, 2916.23) | -1.880 | 0.06 |
| $CD8^+$Cleaved Caspase-$3^+$T-cell ratio (%) | 2.52 (0.82, 4.32) | 0.20 (0.03, 0.89) | -4.195 | <0.001 |
| Cleaved Caspase-3 expression (MFI) in $CD8^+$T cells | 2370.51 (2106.67, 2525.95) | 2564.92 (2224.67, 2914.83) | -0.866 | 0.398 |

Note: MFI (Mean Fluorescence Intensity).

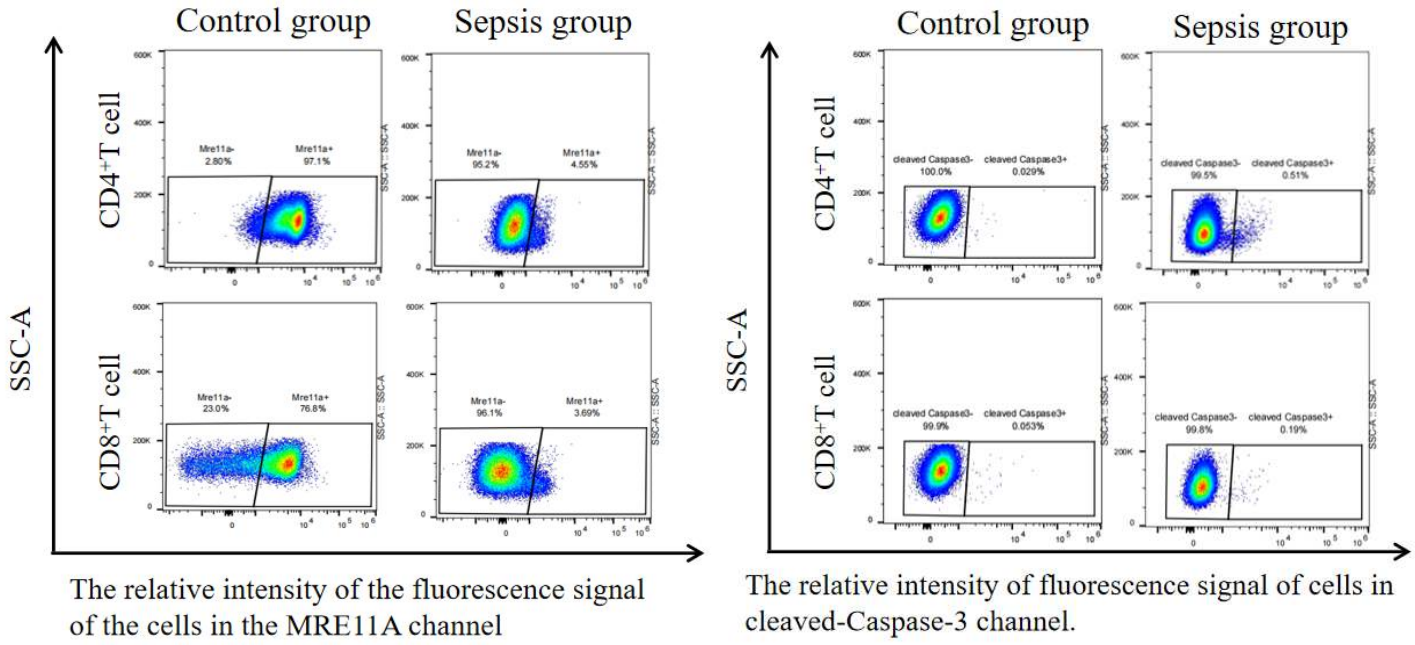



Fig. 1 Changes in MRE11A and Cleaved caspase-3 in the cytoplasm of CD4 + T cells and CD8+ T cells

**Evaluation of the Sepsis Mouse Model**

To evaluate the success of the cecal ligation and puncture (CLP) procedure, we assessed the general condition of mice using the MSS criteria and performed HE staining on mouse lung tissue.Following cecal ligation and puncture modeling, mice in the sepsis group and Mirin group gradually exhibited symptoms including erect hair on the back, reduced feeding and activity frequency, delayed response to sound, increased ocular discharge, and decreased respiratory rate. Some Mirin group mice showed milder symptoms compared to the sepsis group. Normal control mice remained active with normal feeding, while some sham-operated mice exhibited reduced feeding.Results indicated significantly elevated MSS scores and increased lung injury scores in both the sepsis and Mirin groups compared to the normal control and sham surgery groups. Lung injury manifested as thickened alveolar walls, widened alveolar septa, granulocyte infiltration, and hemorrhage visible in some alveoli. Enzyme-linked immunosorbent assay (ELISA) analysis further confirmed this, demonstrating an upward trend in serum interleukin-6 levels.

Table 4 Sepsis Scores for Each Group

| Group | n | MSS |
|---|---|---|
| Normal control group | 6 | 1.17 ± 0.75 |
| Sham Surgery Group | 6 | 2.00±1.79 |
| CLP group | 6 | 22.17±1.72*# |
| Mirin group | 6 | 20.00±1.67*# |
| *F* | | 321.352 |
| *P* | | <0.001 |

Note: *Compared with the normal control group, $P < 0.05$; #Compared with the sham-operated group, $P < 0.05$.

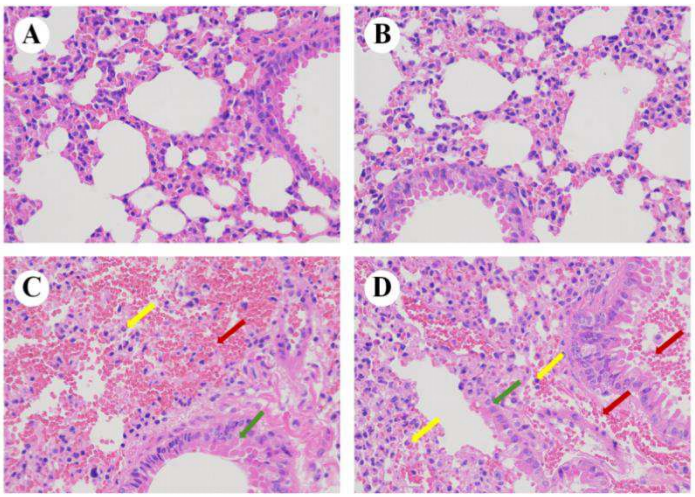
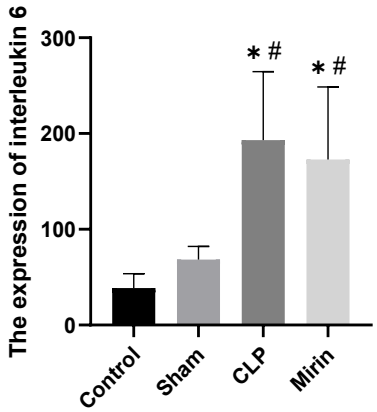



Figure 2 HE staining of lung tissue in each group (400×)

A: Normal control group; B: Sham operation group; C: Sepsis group; D: Mirin group. The green arrow indicates thickened alveolar walls and widened alveolar septa; yellow arrows point to granulocyte or lymphocyte infiltration; the red arrow shows hemorrhage in lung tissue.

Figure 3 Comparison of serum IL-6 levels in each group of mice




### 3.2 MRE11A Expression in T Cells of Sepsis Mice

To investigate MRE11A expression in septic mice, immunofluorescence staining was used to evaluate MRE11A expression in $CD3^{+}$T cells, and Western blotting analyzed MRE11A expression levels in spleen tissue.Immunofluorescence analysis indicated that MRE11A expression in $CD3^{+}$T cells was reduced in the CLP24h group, CLP72h group, and Mirin group of the sepsis group (n=6, $P<0.05$).Western blot analysis showed that MRE11A expression was upregulated in the spleen tissue of the CLP24h group (n=6, $P<0.05$).

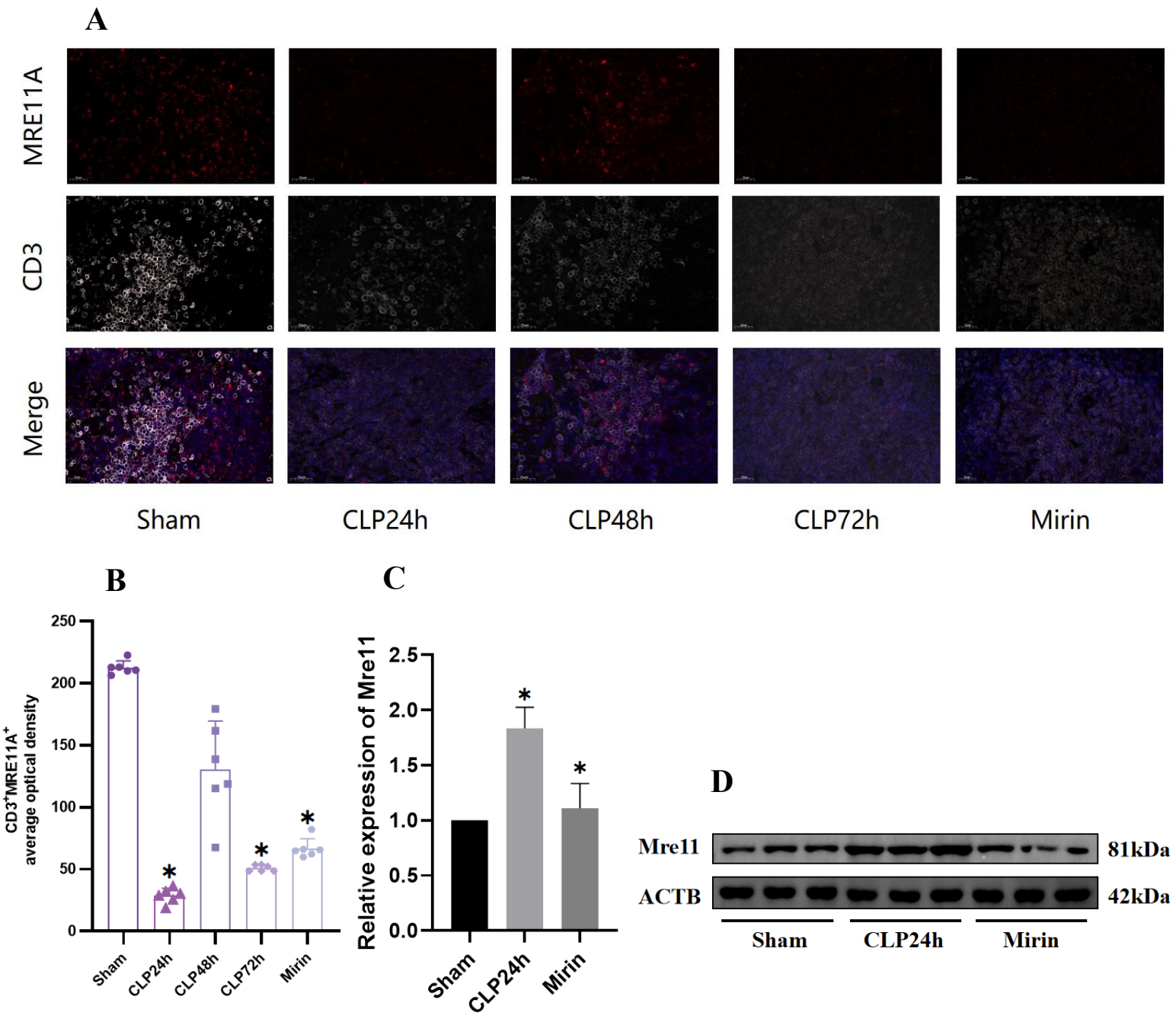


Figure 4 A: Immunofluorescence staining analysis of the Sham group, CLP24h group, CLP48h group, CLP72h group, and Mirin group.

B: Mean fluorescence intensity of MRE11A in $CD3^+$T cells. C and D: Western blot results and quantitative analysis. Data are presented as mean ± standard deviation from at least three independent experiments.

### 3.3 Increased mitochondrial DNA in the cytoplasm of $CD3^+$T cells induced by sepsis

To investigate changes in mitochondrial DNA within the cytoplasm of CD3+ T cells in septic mice, quantitative real-time PCR was performed to detect the relative expression of MT-ND1.Relative MT-ND1 expression was elevated in the CLP24h, CLP48h, CLP72h, and Mirin groups. Expression levels in the control group differed significantly from those in the CLP24h, CLP72h, and Mirin groups (n=6, P<0.05).The difference in expression between the sham-operated group and the CLP24h group was statistically significant ($P < 0.05$), while the difference between the sham-operated group and the normal control group was not statistically significant ($n = 6$, $P > 0.05$).

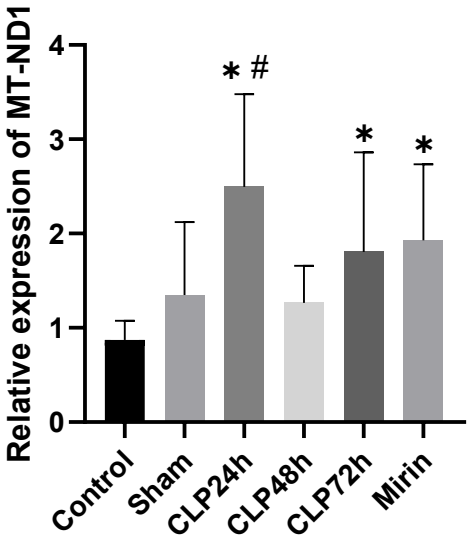



Figure 5 Relative expression of MT-ND1 in spleen T cell cytoplasm of mice in each group

### 3.4 Activation of the STING Pathway Following Sepsis

Given that released mtDNA can activate the STING pathway, we hypothesized that injecting the MRE11A inhibitor Mirin into mice would promote mtDNA release

and thereby activate the STING pathway. To validate this hypothesis, we examined the expression of STING pathway-related factors cGAS and STING in $CD3^{+}$T cells and spleen tissue from mice.

Fluorescent quantitative PCR analysis revealed elevated cGAS expression in the CLP24h, CLP48h, CLP72h, and Mirin groups. Expression levels in the control group differed significantly from those in the CLP24h and Mirin groups. Expression levels in the sham surgery group also differed significantly from those in the CLP24h and Mirin groups.STING expression was elevated in the CLP24h, CLP48h, CLP72h, and Mirin groups. Expression levels in the control and sham surgery groups differed significantly from those in the CLP48h and Mirin groups (all $P < 0.05$).No statistically significant differences were observed between the sham-operated group and the normal control group in the above comparisons. Western blot analysis further confirmed that the CLP24h and Mirin groups significantly upregulated STING protein and its upstream cGAS protein.

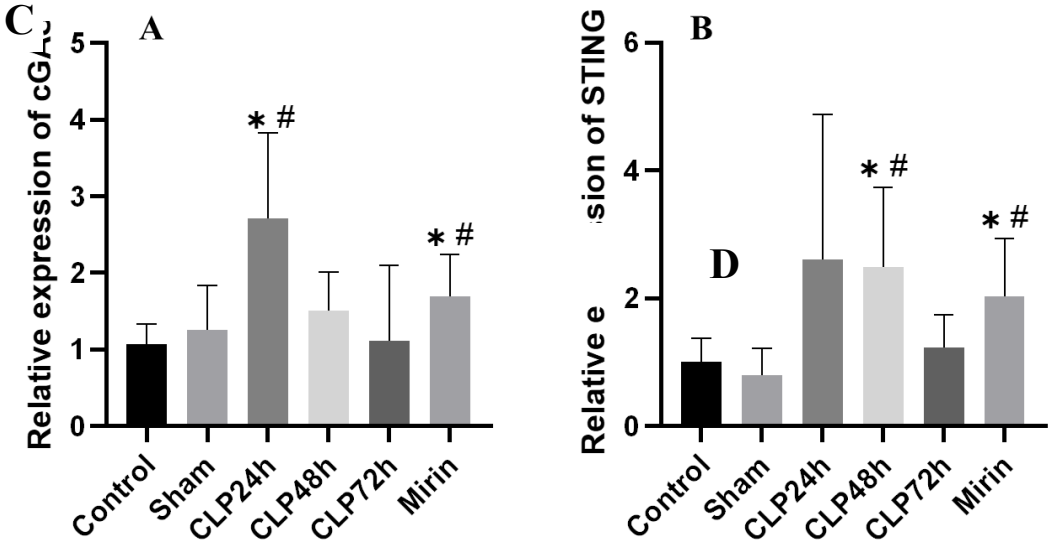
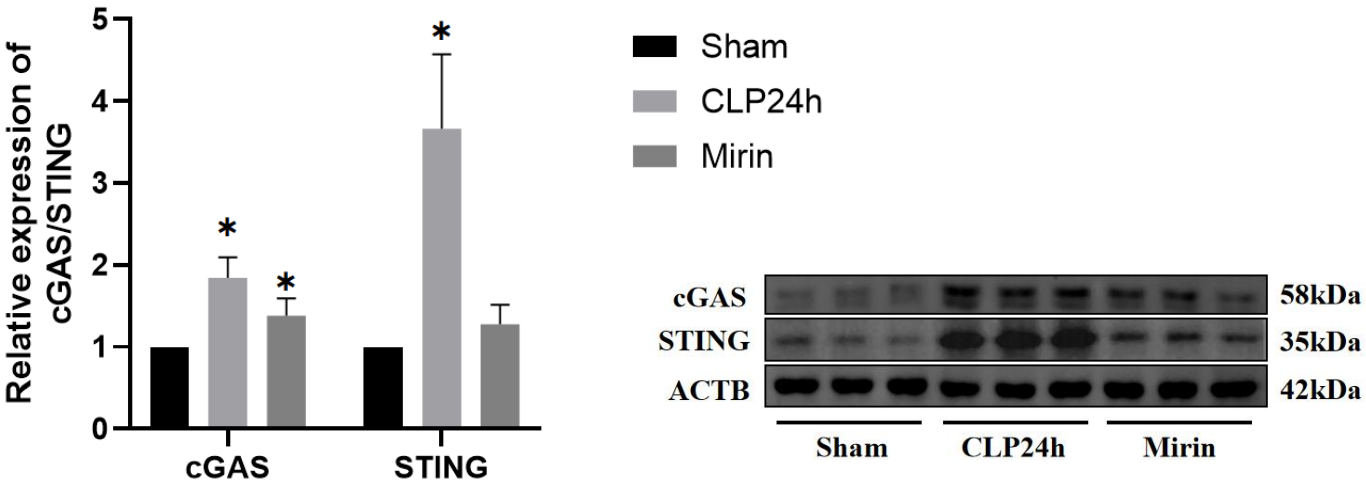



Figure 6 Expression levels of cGAS and STING in splenic T cells from each group




A: Relative expression of cGAS B: Relative expression of STING

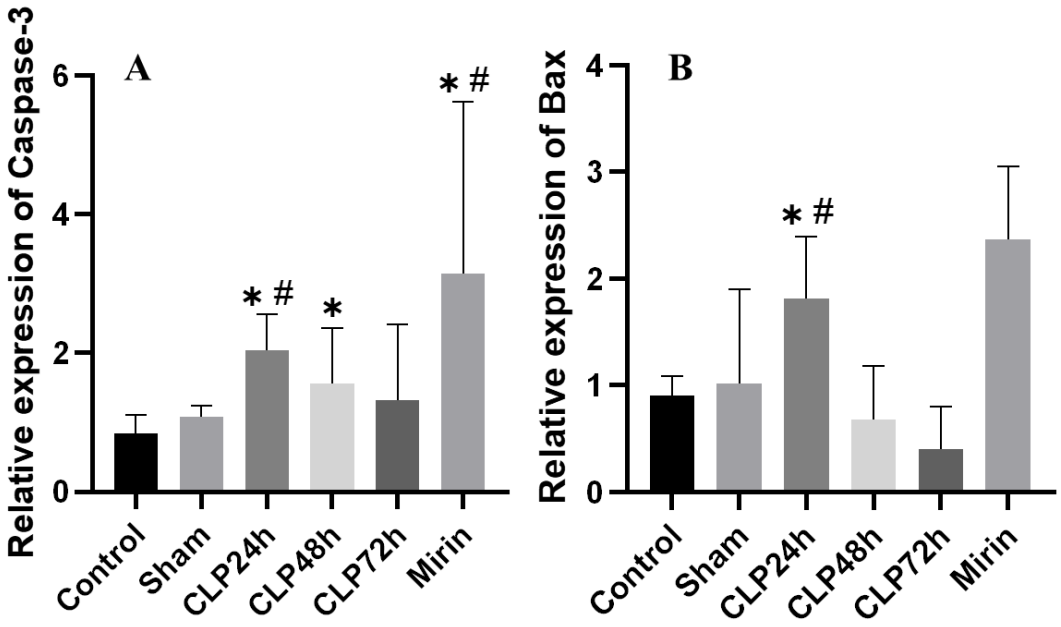
C and D: Western blot results and quantitative analysis. Data are presented as the mean ± standard deviation from at least three independent experiments.

### 3.5 MRE11A may regulate T lymphocyte apoptosis in sepsis via the mtDNA/cGAS/STING pathway

As previously described, the low expression of MRE11A in $CD3^{+}$T cells from the sepsis group may induce mtDNA release, activating the STING pathway. Activation of the STING pathway can induce apoptosis through multiple pathways.To further investigate the relationship between MRE11A and apoptosis, we administered the

MRE11A inhibitor Mirin to mice and analyzed changes in apoptosis-related markers.

Fluorescent quantitative PCR analysis revealed elevated relative expression levels of Cleaved Caspase-3 in the CLP24h, CLP48h, CLP72h, and Mirin groups, with the highest expression observed in the CLP24h group. Expression levels in the control group differed significantly from those in the CLP24h, CLP48h, and Mirin groups ($P < 0.05$).while the sham surgery group showed statistically significant differences compared to the CLP24h, CLP48h, and Mirin groups ($P < 0.05$).The relative expression levels of Bax were elevated in the CLP24h, CLP48h, CLP72h, and Mirin groups. The differences in expression levels between the control group, sham surgery group, and CLP24h group were statistically significant ($P < 0.05$), while the difference between the sham surgery group and the normal control group was not statistically significant ($P > 0.05$).Western blot analysis further confirmed that the CLP24h and Mirin groups significantly upregulated the expression of apoptosis-related factors Bax and Cleaved Caspase-3.



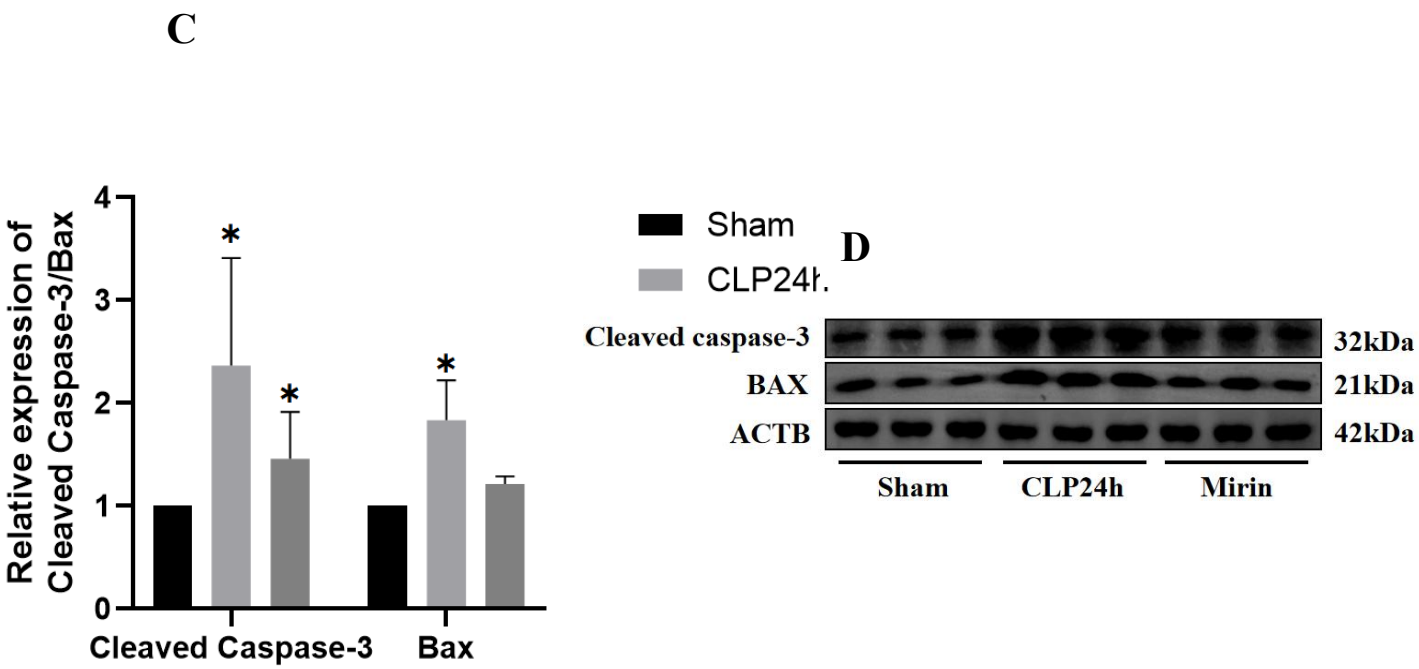



Figure 6 Expression levels of T cell-associated proteins in spleen tissues of mice from different groups: , Cleaved Caspase-3 , and Bax.

A: Relative expression of cleaved caspase-3 B: Relative expression of Bax

C and D: Western blot results and quantitative analysis. Data are presented as the mean ± standard deviation from at least three independent experiments.

## Discussion

Sepsis is a life-threatening multiorgan dysfunction caused by infection-induced dysregulation of host immune responses.Its high mortality rate is closely associated with immune dysregulation, with lymphopenia being a common clinical manifestation of immune abnormalities. Previous studies by our research team have shown that the incidence of lymphopenia in pediatric sepsis patients reaches 47.1%, serving as an independent risk factor for PICU mortality, with patients exhibiting persistent lymphopenia having poorer outcomes. Abnormal apoptosis of immune cells is a major cause of sepsis-associated immunosuppression, with T cell apoptosis being the core pathological mechanism of sepsis-induced immunosuppression.In rheumatoid arthritis, it has been demonstrated that T lymphocytes prematurely age due to MRE11A deficiency. Defective MRE11A in T cells leads to mitochondrial damage, subsequently causing mtDNA repair dysfunction. This repair abnormality ultimately results in

mtDNA leakage from mitochondria into the cytoplasm[6] .However, the expression of MRE11A in sepsis and its mechanism regulating T cell apoptosis remain unclear. In this study, we investigated the expression of MRE11A in T cells during sepsis, its correlation with mitochondrial DNA changes, and the patterns of T cell apoptosis. We preliminarily explored the relationship between mitochondrial DNA leakage in septic T cells, the STING pathway, and T cell apoptosis.Our findings indicate that reduced MRE11A expression in mouse septic T lymphocytes may induce mtDNA leakage, which participates in T lymphocyte apoptosis by activating the STING pathway. These discoveries suggest that MRE11A could emerge as a potential new therapeutic target for clinical treatment of sepsis.

MRE11A is a core component of the DNA damage repair complex MRE11-RAD50-NBS1 (MRN), primarily localized in the nucleus with cytoplasmic expression also observed[6] . It initiates homologous recombination repair[21] It participates in activating the ATM kinase signaling pathway to maintain genomic stability[22] and inhibits tumor cell proliferation[21] , among other functions. Research by Dmitrieva NI et al. indicates that MRE11A is expressed in mammalian mitochondria and binds to mitochondrial DNA[12] .In previous rheumatoid arthritis studies, MRE11A deficiency impaired mitochondrial DNA damage repair. Resulting metabolic abnormalities led to cytoplasmic lipid droplet accumulation, promoting an aggressive T-cell phenotype and ultimately exacerbating joint destruction[23] .Research on Mirin in sepsis animal models remains limited. Our initial study referenced Med Chem Express's Mirin drug label, administering the maximum recommended dose of 20 mg/kg via intraperitoneal injection. However, this failed to significantly mimic reduced MRE11A levels in mice. After adjusting the dose to 25 mg/kg, the simulated reduction in MRE11A became markedly more pronounced.Results indicate that in pediatric sepsis patients, both the proportion of MRE11A-positive cells and expression levels in CD4+ and CD8+ T cells are significantly lower than in healthy children, while expression of the apoptotic molecule Cleaved Caspase-3 is elevated.In animal experiments, $CD11a^{+}$T cells in the sepsis group (CLP24h, CLP72h) and Mirin group showed significantly reduced MRE11A expression ($P<0.05$), whereas no statistical difference was observed in the

CLP48h group. Western blot analysis revealed that MRE11A expression was upregulated in $CD11a^{+}$T cells from the spleen and tissues of the CLP24h group.

Regulation of MRE11 exhibits heterogeneity across different tissue types. In oral squamous cell carcinoma, MRE11A is significantly downregulated, potentially promoting carcinogenesis by impairing DNA damage repair capacity[24] . In prostate cancer, MRE11 and O-GlycNAc accumulate at specific SNP sites, with loss of MRE11 activity leading to a hypermutation phenotype[25] , suggesting that epigenetic regulation may promote tissue-specific overexpression of MRE11. Furthermore, truncated MRE11 is generated by the protease SPRTN, exhibiting impaired nuclease activity and reduced DNA-binding capacity. The presence of this isoform may lead to detection of "high expression" by conventional antibodies, despite actual loss of repair function[26] .In this study, we propose that the reduced expression of MRE11A in the sepsis and Mirin groups primarily correlates with repair defects associated with energy stress. The high expression of MRE11A in spleen tissue relates to increased DNA repair demands and epigenetic regulation. Collectively, these changes reflect the complexity of MRE11's dynamic regulation under pathological conditions.

The mitochondrial-encoded NADH dehydrogenase 1 gene (MT-ND1) is one of the genes encoded by mitochondrial DNA (mtDNA) and constitutes a core subunit of mitochondrial respiratory chain complex I.Mutations or abnormal expression of the MT-ND1 gene can lead to mitochondrial dysfunction, which is associated with various diseases. It holds significant clinical application value in mtDNA testing, particularly in tumor diagnosis[27] and monitoring of mitochondrial diseases[28] . Therefore, the MT-ND1 gene was selected as the target gene for this experiment.In this study, elevated MT-ND1 expression was observed in the sepsis group (CLP24h, CLP72h) and the Mirin group ($P<0.05$), suggesting abnormal release of mtDNA during mitochondrial function. This may be related to reduced mtDNA repair capacity due to MRE11A deficiency, which in turn leads to mitochondrial dysfunction.Recent studies indicate that MRE11 binds the MRN complex to nucleosome fragments, dissociating cGAS from histone acidic fragments. This enables cGAS to bind and be activated by double-stranded DNA[14] . In normal mouse tubular cells, MRE11 colocalizes with

mitochondria, suggesting its involvement in mtDNA stability maintenance[12] .MRE11A is critical for mitochondrial respiratory chain function. In $CD4^+$T cells from rheumatoid arthritis patients, MRE11A deficiency leads to impaired mitochondrial oxygen consumption, reduced ATP production, and severely compromised cellular energy metabolism[29] .Previous studies indicate that MRE11A functions extend beyond nuclear DNA maintenance, significantly participating in mitochondrial function regulation. Combining the findings of downregulated MRE11A expression and elevated MT-ND1 expression, we hypothesize that the downregulation of MRE11A in sepsis induces mtDNA leakage, potentially associated with mitochondrial dysfunction.However, this study only assessed mitochondrial DNA expression levels and lacks further validation of mitochondrial functional changes, such as mitochondrial membrane potential and reactive oxygen species.

Mitochondrial dysfunction promotes the release of mitochondrial DNA into the cytoplasm[30] . As a cytoplasmic DNA sensor, cGAS recognizes free mtDNA and activates the STING pathway, thereby driving type I interferon and pro-inflammatory cytokine expression[31] .MRE11 typically forms a complex with RAD50 (MRE11-RAD50), which not only participates in DNA damage repair but also directly recognizes dsDNA and activates the STING signaling pathway[32] .In grass carp viral infections, the interaction between MRE11 and STING has been clearly demonstrated. MRE11 colocalizes with STING and synergistically activates the expression of interferon and antiviral effector molecules through physical binding[33] . These studies suggest that MRE11 plays a crucial role in antiviral defense by recognizing cytoplasmic dsDNA and synergistically activating innate immune signaling pathways with STING.In this study, cGAS and STING expression significantly increased in the sepsis and Mirin groups ($P$<0.05). Notably, the peak cGAS expression in the CLP24h group aligned with the rising trend of MT-ND1.STING expression peaked in the CLP48h group ($P$<0.05), lagging behind cGAS activation. This discrepancy may stem from two possibilities: first, insufficient sample size potentially compromised statistical power;Second, it may relate to the cascade amplification effect of the STING pathway. As a key mediator of cytoplasmic DNA sensing, STING is activated by cGAMP—a second messenger

synthesized by cGAS—not only within cells containing cytoplasmic DNA but also via gap junctions in neighboring cells[34] . This mechanism enables STING pathway activation to amplify immune responses both locally and systemically.Furthermore, significantly higher STING expression in the Mirin group compared to normal controls ($P$<0.05) suggests that MRE11A inhibition may further activate the STING pathway by exacerbating mtDNA leakage.

Sepsis-induced T cell apoptosis is one of the core mechanisms of immune suppression. Massive apoptosis of $CD4^+$and $CD8^+$T cells directly impairs adaptive immune responses[35]. T cell apoptosis correlates with poor sepsis prognosis[36] .Activation of the STING pathway can induce apoptosis through multiple mechanisms. The B-cell lymphoma 2 gene (Bcl-2) is a key gene in apoptosis research. The Bcl-2-associated X protein (Bax), a Bcl-2 homologous soluble-associated protein, is an apoptosis-promoting gene within the Bcl-2 gene family· .On one hand, mtDNA is released into the cytoplasm through large pores formed by Bax, activating the cGAS/STING pathway to trigger inflammation and apoptosis[38] .STING also promotes the release of inflammatory cytokines such as TNF-α and IL-6 through the NF-κB pathway activated by B-cell κ-light chain enhancement. These factors enhance pro-apoptotic protein Bax expression via the extrinsic apoptosis pathway, inducing cell death[39] .Conversely, STING interacts with endoplasmic reticulum stress to activate the Caspase-3 cascade[40] . Furthermore, mitochondrial membrane potential collapse triggers cytochrome C release, amplifying Caspase-dependent apoptosis[39] .This study selected the apoptotic marker molecules Caspase-3 and Bax for detection. Results indicated that apoptosis-related molecule Caspase-3 expression was significantly upregulated in both the sepsis group and the Mirin group, while Bax expression increased in the sepsis group (both P<0.05). Among these, the CLP24h group exhibited the highest relative expression levels.The sustained activation of the STING pathway in T lymphocytes during sepsis, as observed in this study, parallels the dynamic changes in apoptotic markers, suggesting a crucial role for this pathway in T lymphocyte apoptosis during sepsis.

Previous studies indicate that within 24 to 48 hours after CLP surgery, septic mice

first exhibit a hyperinflammatory response, gradually transitioning to an immunosuppressive state. Abnormal T lymphocyte function is observable early on, such as reduced spleen $CD4^+$T cells and increased Treg proportion detectable within 18 hours post-CLP[41] .PD-1 expression on T cells is upregulated in the early phase of sepsis (24 hours) and persists into the late phase; blocking this pathway reverses immunosuppression.Results from this section indicate that the CLP24h group exhibited the lowest cytoplasmic MRE11A expression in T cells, while MT-ND1 and cGAS expression reached peak levels. Apoptosis-related factors Caspase-3 and Bax expression were also highest among the three CLP group time points, with all differences statistically significant ($P<0.05$).Multiple studies indicate that in CLP-induced sepsis models, immunosuppression typically begins 24 hours post-surgery and peaks between 5-7 days, coinciding with the window for secondary infection. Integrating prior research with these findings, could MRE11A induce mtDNA leakage at CLP24h, activating the STING pathway to maximize T cell apoptosis?The timing of immunosuppression is closely linked to disease progression stages. Could CLP24h-induced sepsis in mice represent an immunosuppressed state? However, factors like ligation length, needle gauge, and puncture frequency influence model severity and reproducibility. Post-CLP bacterial clearance capacity also correlates with Caspase-1 activity, potentially reflecting individual immune variability[42] .All these factors can influence the specific time window. We need to further standardize the model, establish more time points, and detect immunosuppression-related molecules to explore this hypothesis.

This study combines clinical data with animal experiments to preliminarily establish the value of MRE11A in sepsis. It is the first to explore the correlation between low MRE11A expression and T-cell apoptosis and lymphopenia in sepsis, and preliminarily reveals the mediating role of the mtDNA/cGAS/STING pathway.Downregulation of T-cell MRE11A expression in septic mice may induce mtDNA leakage, activate the cGAS/STING pathway, and promote T-lymphocyte apoptosis. This finding provides a novel molecular mechanism for immune suppression in sepsis and lays a theoretical foundation for therapeutic strategies targeting the STING

pathway or MRE11A.Although this study preliminarily reveals the potential mechanism of the MRE11A-STING-apoptosis axis, the following limitations exist: 1. Small sample size in clinical studies. The animal model also had a small sample size, with significant intra-group variability in some data sets, potentially leading to insufficient statistical power; 2. Failure to directly validate MRE11A function at the cellular level through gene knockout or overexpression experiments;3. Regarding the selection of dynamic observation time points, although literature suggests that 24 hours post-modeling may represent a turning point for immune suppression in sepsis, changes were only observed at 24, 48, and 72 hours, lacking earlier dynamic data; 4. The upstream mechanism by which sepsis regulates T-cell MRE11A remains unexplained.

## References


[1] Evans L, Rhodes A, Alhazzani W, et al. Surviving sepsis campaign: international guidelines for management of sepsis and septic shock 2021[J]. Intensive Care Medicine, 2021, 47(11): 1181-1247.

[2] Ying Jia Yun, Liu Ting Yan, Zhou Wen Bin, et al. Interpretation of the 2024 International Consensus Standards: Pediatric Sepsis and Septic Shock [J]. Chinese Journal of Pediatric Emergency Medicine, 2024, 31(05): 322-326.

[3] Chen Jianping, Li Xiaoyue, Fu Ming. Advances in Immunomodulatory Therapy Targeting Immunomodulatory Mechanisms in Sepsis [J]. Medical Review, 2021, 27(13): 2600-2605.

[4] Mithal L B, Arshad M, Swigart L R, et al. Mechanisms and modulation of sepsis-induced immune dysfunction in children[J]. Pediatric Research, 2022, 91(2): 447-453.

[5] Torres L K, Pickkers P, Van Der Poll T. Sepsis-Induced Immunosuppression[J]. Annual Review of Physiology, 2022, 84: 157-181.

[6] Li Y, Shen Y, Jin K, et al. The DNA Repair Nuclease MRE11A Functions as a Mitochondrial Protector and Prevents T Cell Pyroptosis and Tissue Inflammation[J]. Cell Metabolism, 2019, 30(3): 477-492.e6.

[7] Boomer J S, To K, Chang K C, et al. Immunosuppression in patients who die of sepsis and multiple organ failure[J]. JAMA, 2011, 306(23): 2594-2605.

[8] Huang L, Zhang X, Fan J, et al. EGFR promotes apoptosis of CD4+ T lymphocytes through TBK1/Glut1-induced Warburg effect in sepsis[J]. Journal of Advanced Research, 2023, 44: 39-51.

[9] Angus DC, Van Der Poll T. Severe sepsis and septic shock[J]. The New England Journal of Medicine, 2013, 369(9): 840-851.

[10] Paolini A, Borella R, De Biasi S, et al. Cell Death in Coronavirus Infections: Uncovering Its Role during COVID-19[J]. Cells, 2021, 10(7): 1585.

[11] Zahid A, Ismail H, Li B, et al. Molecular and Structural Basis of DNA Sensors in Antiviral Innate Immunity[J]. Frontiers in Immunology, 2020, 11: 613039.

[12] Dmitrieva N I, Malide D, Burg M B. Mre11 is expressed in mammalian

mitochondria where it binds to mitochondrial DNA[J]. American Journal of Physiology. Regulatory, Integrative and Comparative Physiology, 2011, 301(3): R632-640.

[13] Ji W, Zhang L, Ma C, et al. Newly synthesized AIFM1 determines the hypersensitivity of T lymphocytes to STING activation-induced cell apoptosis[J]. Cell Reports, 2023, 42(4): 112327.

[14] Farge G, Falkenberg M. Organization of DNA in Mammalian Mitochondria[J]. International Journal of Molecular Sciences, 2019, 20(11): 2770.

[15] Zhou W, Whiteley A T, De Oliveira Mann C C, et al. Structure of the Human cGAS-DNA Complex Reveals Enhanced Control of Immune Surveillance[J]. Cell, 2018, 174(2): 300-311.e11.

[16] Cho M-G, Kumar R J, Lin C-C, et al. MRE11 liberates cGAS from nucleosome sequestration during tumorigenesis[J]. Nature, 2024, 625(7995): 585-592.

[17] Gulen M F, Koch U, Haag S M, et al. Signaling strength determines proapoptotic functions of STING[J]. Nature Communications, 2017, 8(1): 427.

[18] Li J, Han X, Sun M, et al. Caspase-9 inhibition triggers Hsp90-based chemotherapy-mediated tumor intrinsic innate sensing and enhances antitumor immunity[J]. Journal for Immunotherapy of Cancer, 2023, 11(12): e007625.

[23] Qin H, Lu N, Chen K, et al. Inhibiting caspase-3/GSDME-mediated pyroptosis ameliorates septic lung injury in a mouse model[J]. Molecular Immunology, 2024, 172: 96-104.

[24] Miliaraki M, Briassoulis P, Ilia S, et al. Serum protein levels of survivin and caspase- , and mRNA expression of survivin variants in sepsis[J]. Scientific Reports, 2021, 11(1): 1049.

[25] Liu L, Yan M, Yang R, et al. Adiponectin Attenuates Lipopolysaccharide-induced Apoptosis by Regulating the Cx43/PI3K/AKT Pathway[J]. Frontiers in Pharmacology, 2021, 12: 644225.

[26] Yin H-Y, Wei J-R, Zhang R, et al. Effect of glutamine on caspase-3 mRNA and protein expression in the myocardium of rats with sepsis[J]. The American Journal of the Medical Sciences, 2014, 348(4): 315-318.

[27] Hu Y, Pei Q, Yao M. A study on a sepsis-induced lung injury model in mice[J].

Journal of Bengbu Medical College, 2019, 44(4): 429-433.

[28] Shrum B, Anantha R V, Xu S X, et al. A robust scoring system to evaluate sepsis severity in an animal model[J]. BMC Research Notes, 2014, 7: 233.

[29] Gao R, Singh R, Kaul Z, et al. Targeting of DNA Damage Signaling Pathway Induced Senescence and Reduced Migration of Cancer cells[J]. The Journals of Gerontology. Series A, Biological Sciences and Medical Sciences, 2015, 70(6): 701-713.

[30] Takagi M, Yoshida M, Nemoto Y, et al. Loss of DNA Damage Response in Neuroblastoma and Utility of a PARP Inhibitor[J]. Journal of the National Cancer Institute, 2017, 109(11).

[31] Masoumi M, Alesaeidi S, Khorramdelazad H, et al. Role of T Cells in the Pathogenesis of Rheumatoid Arthritis: Focus on Immunometabolism Dysfunctions[J]. Inflammation, 2023, 46(1): 88-102.

[32] Oliveira Alves M G, Da Silva Miguel N, Ferreira C C P, et al. Expression of DNA repair genes in oral squamous cell carcinoma using reverse transcription-quantitative polymerase chain reaction[J]. Oral Surgery, Oral Medicine, Oral Pathology and Oral Radiology, 2020, 130(3): 298-305.

[33] Gondane A, Girmay S, Helevä A, et al. O-GlcNAc transferase couples MRE11 to transcriptionally active chromatin to suppress DNA damage[J]. Journal of Biomedical Science, 2022, 29(1): 13.

[34] Na J, Newman J A, Then C K, et al. SPRTN protease-cleaved MRE11 decreases DNA repair- s and radiosensitizes cancer cells[J]. Cell Death & Disease, 2021, 12(2): 165.

[35] Warowicka A, Wołuń-Cholewa M, Kwaśniewska A, et al. Alterations in mitochondrial genome in carcinogenesis of HPV-positive cervix[J]. Experimental and Molecular Pathology, 2020, 117: 104530.

[36] Lee J S, Yoo T, Lee M, et al. Genetic heterogeneity in Leigh syndrome: Highlighting treatable and novel genetic causes[J]. Clinical Genetics, 2020, 97(4): 586-594.

[37] Weyand C M, Goronzy J J. Immunometabolism in the development of

rheumatoid arthritis[J]. Immunological Reviews, 2020, 294(1): 177-187.

[38] Zhang JZ. Research progress on the role of mitochondrial dysfunction and mitochondrial DNA release in sepsis-associated acute lung injury[J]. Chinese Critical Care Medicine, 2024, 36(1): 102-105.

[39] Jiménez-Loygorri J I, Villarejo-Zori B, Viedma-Poyatos Á, et al. Mitophagy curtails cytosolic mtDNA-dependent activation of cGAS/STING inflammation during aging[J]. Nature Communications, 2024, 15(1): 830.

[40] Kondo T, Kobayashi J, Saitoh T, et al. DNA damage sensor MRE11 recognizes cytosolic double-stranded DNA and induces type I interferon by regulating STING trafficking[J]. Proceedings of the National Academy of Sciences of the United States of America, 2013, 110(8): 2969-2974.

[41] Xu X, Li M, Deng Z, et al. Grass carp Mre11A activates IFN-1 response by targeting STING to defend against GCRV infection[J]. Developmental and Comparative Immunology, 2021, 116: 103909.

[42] Pépin G, Gantier M P. cGAS-STING Activation in the Tumor Microenvironment and Its Role in Cancer Immunity[J]. Advances in Experimental Medicine and Biology, 2017, 1024: 175-194.

[43] Lu G, Li Q, Liu J, et al. Inhibition of endoplasmic reticulum stress and the downstream pathways protects CD4+ T cells against apoptosis and immune dysregulation in sepsis[J]. IUBMB Life, 2022, 74(11): 1070-1080.

[44] W ang Z, Xie Z, Zhao Y, et al. Effect of dendritic cells on immune function regulated by programmed cell death-1/programmed cell death-ligand 1 in sepsis. Chinese Journal of Immunology, 2021, 33(9): 1032-1039.

[45] Amarasiri H A. D B, Arachchige D, Vince M J K, et al. Inhibitory Potential and Binding Thermodynamics of Scyllatoxin-Based BH3 Domain Mimetics Targeting Repressor BCL2 Proteins[J]. Journal of Molecular Recognition: JMR, 2025, 38(2): e70001.

[46] Zhou Z, Xu L, Lv Y, et al. BAX pores facilitate mitochondrial DNA release in wasp sting-induced acute kidney injury[J]. International Immunopharmacology, 2024, 143(Pt 2): 113424.

[47] Tao H, Luo J, Wen Z, et al. [High STING expression exacerbates renal ischemia-reperfusion injury in mice by regulating the TLR4/NF-κB/NLRP3 pathway and promoting inflammation and apoptosis][J]. Journal of Southern Medical University, 2024, 44(7): 1345-1354.

[48] Soh L-J, Lee S-Y, Roebuck M M, et al. Unraveling the interplay between ER stress, UPR, and the cGAS-STING pathway: Implications for osteoarthritis pathogenesis and treatment strategy[J]. Life Sciences, 2024, 357: 123112.

[49] Chen J, Chen R, Huang S, et al. Atezolizumab alleviates the immunosuppression induced by PD-L1-positive neutrophils and improves the survival of mice during sepsis[J]. Molecular Medicine Reports, 2021, 23(2): 144.

[50] Durand M, Hagimont E, Louis H, et al. The β 1 -Adrenergic Receptor Contributes to Sepsis-Induced Immunosuppression Through Modulation of Regulatory T-Cell Inhibitory Function[J]. Critical Care Medicine, 2022, 50(9): e707-e718.

[51] Phares TW, Kotraiah V, Chung CS, et al. A Peptide-Based Checkpoint Immunomodulator Alleviates Immune Dysfunction in Murine Polymicrobial Sepsis[J]. Shock (Augusta, Ga.), 2021, 55(6): 806-815.

[52] Shang Shenglan. Molecular Mechanism Study of Artemisinin Derivative Luteo's Protective Effect on Sepsis-Induced Immunodeficiency in Mice[D]. Army Medical University, People's Liberation Army of China, 2021.

[53] De Lima M H F, Hiroki C H, De Fátima Borges V, et al. Sepsis-Induced Immunosuppression Is Marked by an Expansion of a Highly Suppressive Repertoire of FOXP3+ T-Regulatory Cells Expressing TIGIT[J]. The Journal of Infectious Diseases, 2022, 225(3): 531-541.

[54] Yuan Y, Hua L, Zhou J, et al. The effect of artesunate to reverse CLP-induced sepsis immunosuppression in mice with secondary infection is tightly related to reducing T cell apoptosis via decreasing inhibitory receptors and activating the MAPK/ERK pathway[J]. International Immunopharmacology, 2023, 124(Pt A): 110917.

[55] Alverdy JC, Keskey R, Thewissen R. Can the Cecal Ligation and Puncture Model Be Repurposed To Better Inform Therapy in Human Sepsis?[J]. Infection and

Immunity, 2020, 88(9): e00942-19.

## Declarations

**Ethics Approval:** Studies involving human subjects and animals were approved by the Medical Ethics Committee of the First Affiliated Hospital of Guangxi Medical University (Approval No. 2023-E031-01). All studies were conducted in accordance with relevant local laws, regulations, and institutional requirements. The Ethics Committee waived the requirement for written informed consent from the subjects or their legal guardians/next of kin due to the retrospective nature of the clinical study.

Consent for Publication: Not applicable.

**Availability of Data and Materials:** The datasets generated and/or analyzed during the current study are available from the corresponding author on reasonable request.

Competing Interests: The authors declare no competing interests.

**Funding:** This research was funded by the Guangxi Clinical Research Center for Pediatric Diseases (Project No. GUIKEAD22035219) and the Guangxi Natural Science Foundation General Program (Project No. 2024GXNSFAA010084).

**Authors' Contributions:** ZW: Writing – original draft. FW: Data curation, Writing – original draft. QP: Experimental design – original draft. ZY: Writing – review & editing. All authors read and approved the final manuscript.

**Acknowledgements:** Guangxi Clinical Research Center for Pediatric Diseases